0013-7227/08/$15.00/0
Printed in U.S.A.

Endocrinology 149(6):3077–3084

doi: 10.1210/en.2008-0027

Molecular Characterization of V59E NIS, a Na^+/I^- Symporter Mutant that Causes Congenital I^- Transport Defect

Mia D. Reed-Tsur, Antonio De la Vieja, Christopher S. Ginter, and Nancy Carrasco

Department of Molecular Pharmacology, Albert Einstein College of Medicine, Bronx, New York 10461

I^- is actively transported into thyrocytes via the Na^+/I^- symporter (NIS), a key glycoprotein located on the basolateral plasma membrane. The cDNA encoding rat NIS was identified in our laboratory, where an extensive structure/function characterization of NIS is being conducted. Several NIS mutants have been identified as causes of congenital I^- transport defect (ITD), including V59E NIS. ITD is characterized by low thyroid I^- uptake, low saliva/plasma I^- ratio, hypothyroidism, and goiter and may cause mental retardation if untreated. Studies of other ITD-causing NIS mutants have revealed valuable information regarding NIS structure/function. V59E NIS was reported to exhibit as much as 30% of the activity of wild-type NIS. However, this observation was at variance with the patients' phenotype of total lack of activity. We have thoroughly characterized V59E NIS and studied several amino acid substitutions at position 59. We demonstrated that, in contrast to the previous report, V59E NIS is inactive, although it is properly targeted to the plasma membrane. Glu and all other charged amino acids or Pro at position 59 also yielded nonfunctional NIS proteins. However, I^- uptake was rescued to different degrees by the other substitutions. Although the K_m values for Na^+ and I^- were not altered in these active mutants, we found that the structural requirement for NIS function at position 59 is a neutral, helix-promoting amino acid. This result suggests that the region that contains V59 may be involved in intramembrane helix-helix interactions during the transport cycle without being in direct contact with the substrates. (*Endocrinology* 149: 3077–3084, 2008)

IODIDE (I^-) IS AN ESSENTIAL component of the thyroid hormones T_3 and T_4, which are required for development and maturation of the central nervous system, skeletal muscle, and lungs of the fetus and the newborn and for intermediary metabolism in virtually all tissues (1). The Na^+/I^- symporter (NIS), a highly specialized glycoprotein located on the basolateral membrane of the thyroid epithelial cells, couples the inward translocation of two Na^+ down their electrochemical gradient to the simultaneous inward translocation of one I^- against its electrochemical gradient (2). The driving force for NIS activity is the Na^+ gradient generated by the Na^+/K^+ ATPase.

For decades, I^- uptake in the thyroid has been used for the diagnosis and treatment of several thyroid conditions. However, the molecular analysis of NIS only started in 1996, when our group identified the cDNA that encodes rat NIS (rNIS) (3). In addition to the thyroid, NIS is also expressed in other tissues such as the salivary and lactating mammary glands and gastric mucosa (4, 5). NIS expression in the lactating mammary gland is responsible for transporting I^- into the milk, thus enabling the nursing infant to produce his/her own thyroid hormones (6).

Congenital I^- transport defect (ITD) is a rare autosomal recessive disease defined by a lack of I^- transport (and therefore an absence of thyroid hormones) and, when untreated, characterized by hypothyroidism, goiter, mental retardation, and a diminished saliva/plasma I^- ratio (4, 7). With the isolation of the NIS cDNA, the identification and molecular characterization of mutant NIS molecules that cause ITD became feasible. To date, 12 ITD-causing NIS mutations have been reported (V59E, G93R, R124H, ΔM143-Q323, Q267E, C272X, T354P, G395R, ΔA439-P443, frame-shift 515X, Y531X, and G543E) (8–18) (Fig. 1). Several of these have been thoroughly characterized in our laboratory, yielding important information on NIS structure/function (19–22). Thus, the analysis of T354P NIS (22) led not only to the conclusion that an amino acid with a hydroxyl group at its β-carbon at position 354 is necessary for NIS function but also to the finding that other amino acids within transmembrane segment (TMS) IX (the segment with the highest incidence of amino acids with hydroxyl groups at β-carbons) have the same requirement for NIS function. This observation, in turn, provided the basis for the identification of residues that may be involved in the Na^+ translocation pathway (23). The characterization of the G395R NIS mutant showed that NIS activity requires a small, uncharged amino acid at position 395 (21). We reported that Q267E NIS is properly targeted to the plasma membrane but only transports modest amounts of I^- because of a decrease in the NIS kinetic turnover number (19). In contrast, we determined that G543E NIS does not fully mature and is retained intracellularly as a result of the charge and size of Glu (20).

The V59E NIS mutation was discovered as a compound heterozygous mutation in all three children of a Japanese couple in 2000 (10). The parents themselves had no thyroid dysfunction. This family was first described in 1977 (24),

First Published Online March 13, 2008

Abbreviations: ClO_4^-, perchlorate; HBSS, Hanks' buffered salt solution; ITD, I^- transport defect; NHS-SS-biotin, succinimidyl 2-(biotinamido)-ethyl-1,3′-dithiopropionate-biotin; NIS, Na^+/I^- symporter; rNIS, rat NIS; TMS, transmembrane segment; WT, wild type.

***Endocrinology* is published monthly by The Endocrine Society (http://www.endo-society.org), the foremost professional society serving the endocrine community.**

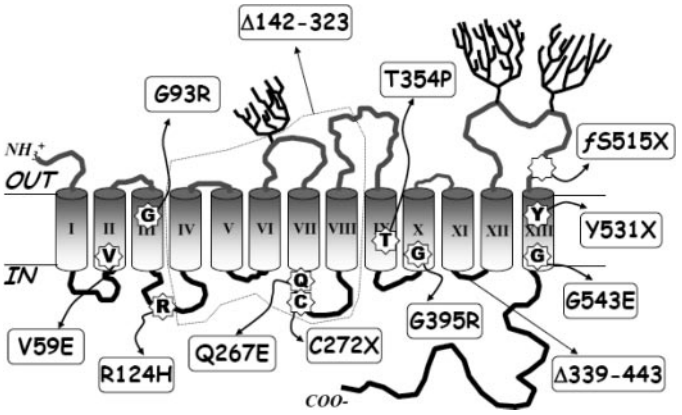

FIG. 1. Schematic representation of the NIS secondary structure model. The current secondary structure model of NIS depicts 13 TMS (labeled with *Roman numerals*) with an extracellular N and a cytosolic C terminus. The 12 ITD-causing NIS mutations are indicated by the single-letter amino acid code, showing the WT residue followed by the position number and the substituted residue. FS, Frame shift; X, premature stop codon; Δ, deletion.

before the molecular identification of NIS. After the NIS cDNA was isolated (3, 25), Fujiwara *et al.* (10) determined in their 2000 study that the patients inherited the T354P and V59E NIS mutations from their mother and father, respectively. That all three siblings had this genotype is remarkable, given the 1/64 likelihood in a normal Mendelian inheritance. Amino acid 59 is located on the cytosolic side of putative TMS II, a region of NIS that is well conserved in all species in which NIS has been sequenced and throughout the SLC5A transporter family, suggesting that this residue plays a role in NIS structure and/or I^- transport (26). Fujiwara *et al.* (10) transfected cDNA constructs encoding V59E and reported that I^- transport in cells expressing V59E NIS was almost 30% of that exhibited by wild-type (WT) NIS. The authors concluded from these data that V59E NIS was not completely inactive, even though this notion is in conflict with the clinical data indicating no activity (saliva/plasma I^- ratios of ~1). In addition, the study lacked the negative controls (*i.e.* transport in the presence of the inhibitor ClO_4^- or in the absence of Na^+) needed to support their conclusions. Hence, to determine to what extent and by what mechanism the V59E substitution disrupts NIS function, we have carried out a thorough molecular characterization of V59E NIS using a variety of methods, including flow cytometry, I^- transport assays, immunoblot, immunofluorescence, and cell surface biotinylation.

Materials and Methods

Site-directed mutagenesis

Site-directed mutagenesis was performed using the following oligos: V59A, GCA GCC GTT CCT SCG GGG CTG TCG; V59D, GCA GCC GTT CCT RAC GGG CTG TCG; V59E, GCA GCC GTT CCT SAG GGG CTG TCG; V59I, GCA GCC GTT CCT ATT GGG CTG TCG CTG; V59K, GCA GCC GTT CCT ARG GGG CTG TCG; V59L, GCA GCC GTT CCT CTG GGG CTG TCG CTG; V59M, GCA GCC GTT ATG GGG CTG TCG CTG; V59N, GCA GCC GTT CCT RAC GGG CTG TCG; V59P, GCA GCC GTT CCT SCG GGG CTG TCG; V59Q, GCA GCC GTT CCT SAG GGG CTG TCG; V59R, GCA GCC GTT CCT ARG GGG CTG TCG; V59T, GCA GCC GTT CCT ACG GGG CTG TCG CTG; and the T354P oligo was the same as in Levy *et al.* (22). Site-directed mutagenesis was carried out as previously described (27). The initial PCR extensions were performed using reverse primers complementary to the 3′ end. These fragments were gel purified and used for a second round of PCR extension with primers complementary to the 5′ end. Fragments with the mutant sequences were obtained by digestion of the final PCR products with the appropriate unique restriction enzyme to obtain the smallest mutant fragments. These fragments were then ligated into WT NIS cDNA (PSVSport-rNIS), and the mutant inserts were sequenced past their respective cloning sites.

Cell culture and transient transfection of COS-7 cells

COS-7 cells were grown at 37 C with 5% CO_2 and maintained in DMEM before transient transfection with 4 μg/plate rat NIS cDNA constructs using Lipofectamine Plus (Invitrogen, Carlsbad, CA) following the manufacturer's instructions. Transfected cells were split 24 h after transfection and analyzed by immunoblot, surface biotinylation, and immunofluorescence, assayed for I^- uptake, and measured by FACS to measure transfection efficiency 48 h after transfection.

Immunoblot analysis

Transiently transfected cells were lysed by incubating them with complete lysis buffer [1% SDS, 50 mM Tris (pH 7.4), 150 mM NaCl, 5 mM EDTA, and 1% Triton X-100] and then adding lysis buffer (complete lysis buffer without SDS) at a dilution of 1:10. After cell lysis, the protein concentration was quantified using the BCA protein measurement kit (Pierce, Rockford, IL). Samples were diluted with sample buffer and incubated at 37 C for 30 min followed by 9% SDS-PAGE, electroblotted to a nitrocellulose membrane, and immunoblotted with 2 nM of an affinity-purified anti-rNIS polyclonal antibody (directed against the last 16 amino acids of the rNIS C terminus) for 1 h and then incubated for 45 min with the antirabbit HRP secondary antibody (Jackson Laboratory, Bar Harbor, ME).

Cell surface biotinylation

Biotinylation of cell surface proteins was performed as previously described (19). Twenty-four hours after transfection, COS-7 cells were split into 12-well plates and maintained in DMEM for 24 h more. Transiently transfected cells were incubated with 1 mg/ml of the membrane-impermeable biotin reagent sulfo-succinimidyl 2-(biotinamido)-ethyl-1,3′-dithiopropionate-biotin (sulfo-NHS-SS-biotin) (Pierce), which covalently interacts with extracellular primary amines. The reaction was subsequently quenched with 100 mM glycine in PBS supplemented with 1 mM $MgCl_2$ and 0.1 mM $CaCl_2$. Cells were lysed and biotinylated proteins precipitated overnight with streptavidin-coated beads, heated with sample buffer containing 100 mM final dithiothreitol at 75 C for 5 min, subjected to SDS-PAGE, and immunoblotted with anti-rNIS. As a control, supernatants obtained after the overnight incubation were analyzed by immunoblot.

Steady-state I^- transport analysis

Transfected cells were assayed under steady-state conditions in triplicate. Forty-eight hours after transfection, cells were washed twice in Hanks' buffered salt solution (HBSS) [140 mM NaCl, 5.4 mM KCl, 1.3 mM $CaCl_2$, 0.4 mM $MgSO_4$, 0.5 mM $MgCl_2$, 0.4 mM $NaHPO_4$, 0.44 mM KH_2PO_4, and 5.55 mM glucose in 10 mM HEPES (pH 7.5)]. Cells were then incubated with 20 μM $K^{125}I$ (specific activity 100 mCi/mmol) and 140 mM Na^+ (unless otherwise indicated) for 45 min to 1 h at 37 C in a humidified atmosphere with 5% CO_2 and then washed twice more with HBSS (4 C). Accumulated I^- was released by incubating cells with 100% ethanol for at least 20 min at 4 C and quantitated in a γ-counter (Perkin-Elmer, Norwalk, CT). I^- uptake was standardized by determining the amount of DNA per well by incubating cells with 5% trichloroacetic acid for 30 min at 4 C followed by an overnight incubation with diphenylamine solution.

I^-- and Na^+-dependent kinetic analysis

For I^--dependent kinetic analysis, cells were incubated with I^- concentrations ranging from 0.6–80 μM $Na^{125}I$ and 140 mM NaCl for 2 min.

Initial rates of I^- transport measured during kinetic analysis were analyzed by nonlinear regression using the following equation: $v([I^-]) = (V_{max} \times [I^-])/(K_m + [I^-]) + A \times [I^-] + B$. The terms A and B refer to background adjusted by least squares of the data obtained with nontransfected cells. For the Na^+-dependent kinetic analysis, cells were incubated with 20 μM $Na^{125}I$ and a range of Na^+ concentrations between 0 and 140 mM for 2 min (isotonicity was maintained using choline-Cl). The equation used to analyze the initial rates is $v([Na^+]) = (V_{max} \times [Na^+]^2)/(K_m^2 + [Na^+]^2) - A \times [Na^+] + B$. Data were analyzed by gnuplot (www.gnuplot.info).

Results

V59E NIS is expressed but inactive

To assess the transport properties of V59E NIS, we measured Na^+-dependent, perchlorate (ClO_4^-)-inhibitable (*i.e.* NIS-mediated) I^- transport at 20 μM I^- and 140 mM Na^+ for 1 h in COS-7 cells expressing either V59E NIS or WT NIS. WT NIS-expressing cells accumulated 80–100 pmol $I^-/\mu g$ DNA; I^- uptake was inhibited by 40 μM ClO_4^-. Cells expressing V59E NIS showed no I^- transport, just like nontransfected COS-7 cells (Fig. 2A). FACS analysis revealed that the transfection efficiency of WT and V59E NIS was similar (data not shown). Cell lysates from transfected COS-7 cells were subjected to SDS-PAGE and immunoblotted with a high-affinity anti-rNIS antibody. NIS expression levels were similar in cells transfected with WT or V59E NIS (Fig. 2B), each expressing the characteristic fully glycosylated mature (~110 kDa) and the partially glycosylated immature polypeptide (~55 kDa). In contrast, no polypeptides were detected in cell lysates from nontransfected COS-7 cells, which do not express endogenous NIS. The endogenously expressed α-subunit of the Na^+/K^+ ATPase was used as a loading control (Fig. 2B).

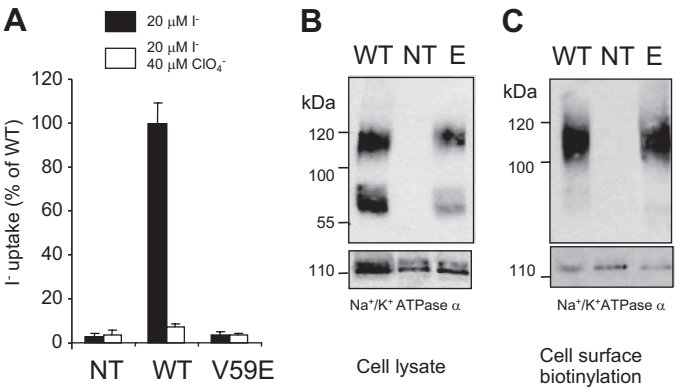

FIG. 2. Characterization of activity and expression of V59E NIS in COS-7 cells. A, Steady-state I^- uptake analysis in nontransfected (NT) COS-7 cells or cells transfected with either WT or V59E NIS was determined. Cells were incubated for 1 h in HBSS containing 140 mM Na^+ and 20 μM $^{125}I^-$ (*black bars*) or HBSS containing 140 mM Na^+ and 20 μM $^{125}I^-$ and 40 μM ClO_4^- (*white bars*); accumulated I^- was measured in a γ-counter and standardized by micrograms of DNA. NT cells represent background levels of I^- transport. Values are expressed as a percentage of the activity of WT NIS (typically 80–100 pmol $I^-/\mu g$ DNA). Values represent the average of at least three different experiments; in each experiment, transport measurements were performed in triplicate. B, Immunoblot analysis. Cell lysates (2 μg) from nontransfected (NT) cells or cells transfected with either WT NIS or V59E NIS (E) were electrophoresed, electrotransferred, and immunoblotted with 2 nM anti-rNIS. C, Cell surface biotinylation. Transfected cells were incubated with the membrane-impermeable sulfo-NHS-SS-biotin reagent (1 mg/ml) and precipitated overnight with streptavidin beads. Streptavidin beads and bound biotinylated proteins were heated in sample buffer at 75 C, and the cell surface biotinylated proteins were immunoblotted with 2 nM anti-rNIS. The α-subunit of the Na^+/K^+ ATPase was used as a loading control (B and C, *bottom panels*).

V59E NIS is properly targeted to the plasma membrane

Whereas the lack of I^- transport mediated by the expressed V59E NIS protein (Fig. 2) suggested that it is inherently incapable of transporting I^-, it was also possible that V59E NIS was not targeted to the plasma membrane. Indeed, previous analysis of other ITD-causing NIS mutants revealed a lack of I^- transport due to improper targeting of the mutant NIS proteins to the cell surface (20). Therefore, we assessed the presence of V59E NIS in the plasma membrane by cell surface biotinylation. Transfected COS-7 cells were treated with sulfo-NHS-SS-biotin, a membrane-impermeable biotin reagent that covalently interacts with extracellular primary amines. Immunoblot analysis of the biotinylated cell surface proteins in cells transfected with WT NIS showed a maturely glycosylated NIS polypeptide, represented by a broad band at about 110 kDa, indicating that, as expected, WT NIS is properly processed and targeted to the cell surface, where it mediates I^- uptake. V59E NIS was also properly targeted to the plasma membrane. The endogenously expressed α-subunit of the Na^+/K^+ ATPase was used as a loading control. In contrast, the soluble protein tubulin was not biotinylated (data not shown). Therefore, the observed lack of I^- transport is not due to improper protein maturation or faulty trafficking to the plasma membrane (Fig. 2C).

The presence of charged amino acids or Pro at position 59 of NIS renders the protein inactive

One possible explanation for the inactivity of the V59E NIS protein is the presence of the negatively charged side chain of Glu instead of the neutral side chain of Val at position 59. Thus, we substituted Val with other charged amino acids (Asp, Arg, and Lys). In addition, we also evaluated the effect of Pro, an α-helix breaker, at position 59. None of the NIS mutants with a charged residue or Pro at position 59 displayed I^- transport (Fig. 3A), even though all (except the Pro mutant) were expressed at levels similar to those of WT NIS (Fig. 3B) and all were properly targeted to the plasma membrane, as determined by cell surface biotinylation (Fig. 3C). The endogenously expressed α-subunit of the Na^+/K^+ ATPase was used as a loading control. These results show that the presence of a charged amino acid or a Pro at position 59 renders NIS inactive.

Neutral amino acids at position 59 rescue NIS activity

The neutral amino acids Ala, Asn, Gln, Ile, Leu, Met, and Thr were individually substituted instead of Val at position 59. Each of the resulting NIS mutant proteins displayed I^- transport at different levels, all significant but lower than those of WT NIS (Fig. 4A). Interestingly, mutants with amino acids at position 59 that had, like Val, branched side chains at the β-carbon (*i.e.* Ile and Thr) exhibited I^- transport at levels comparable to those of WT NIS, independently of the

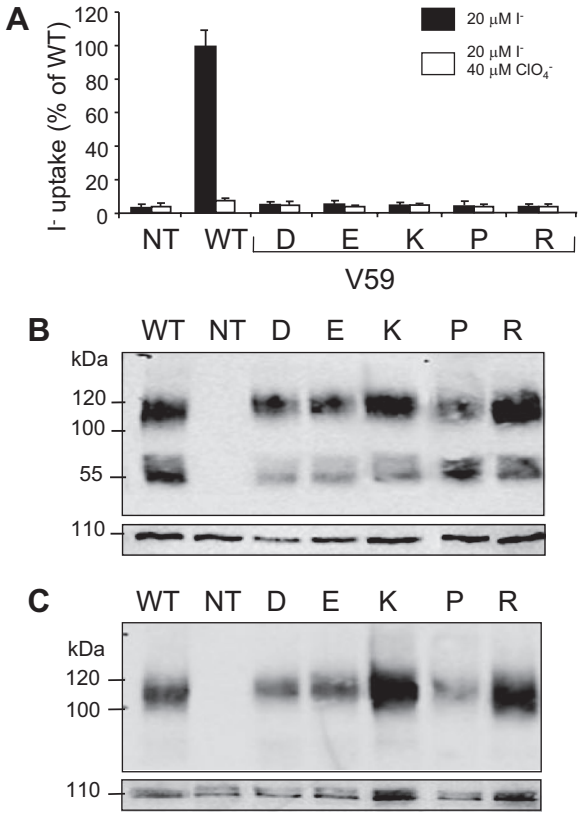

FIG. 3. NIS is inactive with charged amino acids or Pro at position 59 despite proper expression and plasma membrane targeting. COS-7 cells were transfected with WT, V59D, V59E, V59K, V59P, or V59R NIS and analyzed as follows. A, Steady-state I^- transport in cells incubated with 20 μM I^- and 140 mM Na^+ (*black bars*) and in cells incubated with 20 μM I^-, 140 mM Na^+, and 40 μM ClO_4^- (*white bars*). Values are expressed as a percentage of WT NIS activity (typically 80–100 pmol I^-/μg DNA). B, Immunoblot analysis. C, Cell surface biotinylation. The α-subunit of the Na^+/K^+ ATPase was used as a loading control (B and C, *bottom panels*).

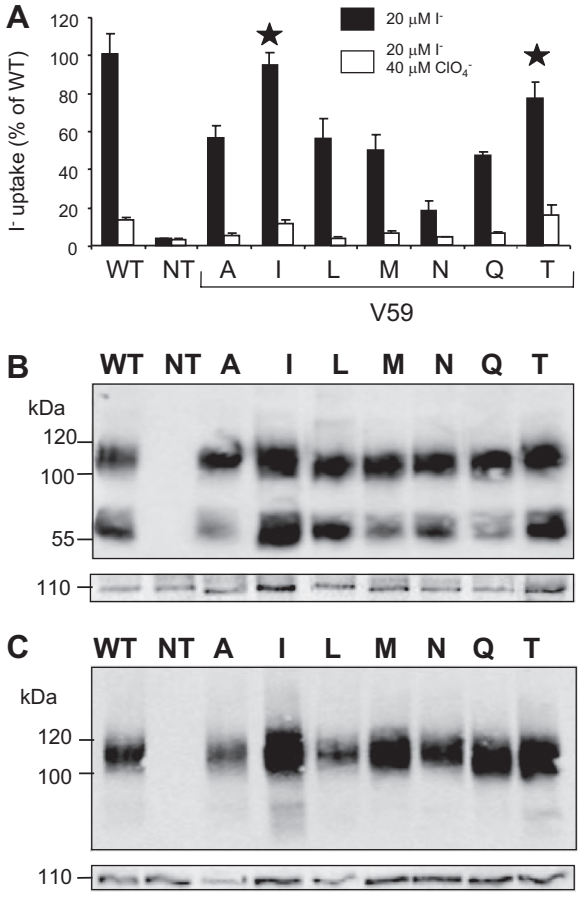

FIG. 4. NIS is active with neutral amino acids other than Pro at position 59. COS-7 cells were transfected with V59A, I, L, M, N, Q, T, or WT NIS cDNAs and analyzed as follows. A, Steady-state I^- transport in cells incubated with 20 μM I^- and 140 mM Na^+ (*black bars*) or 20 μM I^-, 140 mM Na^+, and 40 μM ClO_4^- (*white bars*). *Stars* indicate the amino acid substitutions that are branched at the β-carbon (as Val is), which yield the proteins that mediate the highest levels of I^- accumulation compared with WT NIS. B, Immunoblot analysis. C, Cell surface biotinylation. The α-subunit of the Na^+/K^+ ATPase was used as a loading control (B and C, *bottom panels*).

residue side-chain volume. Each of these NIS mutants was normally expressed after transfection into COS-7 cells (Fig. 4B), and each was also correctly targeted to the plasma membrane, as shown by cell surface biotinylation (Fig. 4C). The endogenously expressed α-subunit of the Na^+/K^+ ATPase was used as a loading control.

The decreased I^- transport in NIS mutants with neutral amino acid substitutions at position 59 is due to a change in V_{max}

We performed kinetic analyses of those NIS mutants that displayed I^- transport (*i.e.* those containing Ala, Asn, Ile, Leu, Met, Gln, or Thr at position 59) to determine whether or not the change in I^- transport with respect to WT NIS was due to a decrease in the apparent affinity of NIS for Na^+ or I^- (as reflected by a change in the respective K_m values) or to a lower NIS kinetic turnover number (as reflected by a change in the V_{max}). Cells were incubated with different concentrations of I^- (ranging from 0.6–80 μM) and 140 mM Na^+ for 2 min to measure the initial rates of I^- transport (Fig. 5A). Na^+-dependent kinetic experiments with the same NIS mutants using Na^+ concentrations from 0–140 mM and 20 μM I^- were also performed to measure initial I^- transport rates as a function of the Na^+ concentration (Fig. 5B). In both cases, each mutant protein exhibited K_m values similar to those of WT NIS but a lower V_{max} (Fig. 5C). Therefore, decreased transport in these mutants results from a lower NIS kinetic turnover.

The V59E/T354P NIS compound mutation is inactive

After demonstrating that V59E NIS is inactive, we decided to experimentally test the compound V59E/T354P NIS mutation because it is expressed in the three Japanese patients. To properly assess I^- uptake mediated by V59E/T354P NIS in relation to that mediated by WT NIS, we cotransfected 2 μg V59E and 2 μg T354P NIS cDNA into COS-7 cells and compared it with transport in cells transfected with 2 or 4 μg WT, V59E, or T354P NIS cDNA. In contrast to the results from Fujiwara *et al.* (10), who reported that V59E/T354P NIS exhibited approximately 20% of WT NIS I^- transport levels, we observed no I^- accumulation mediated by the compound mutant. Transfection ef-

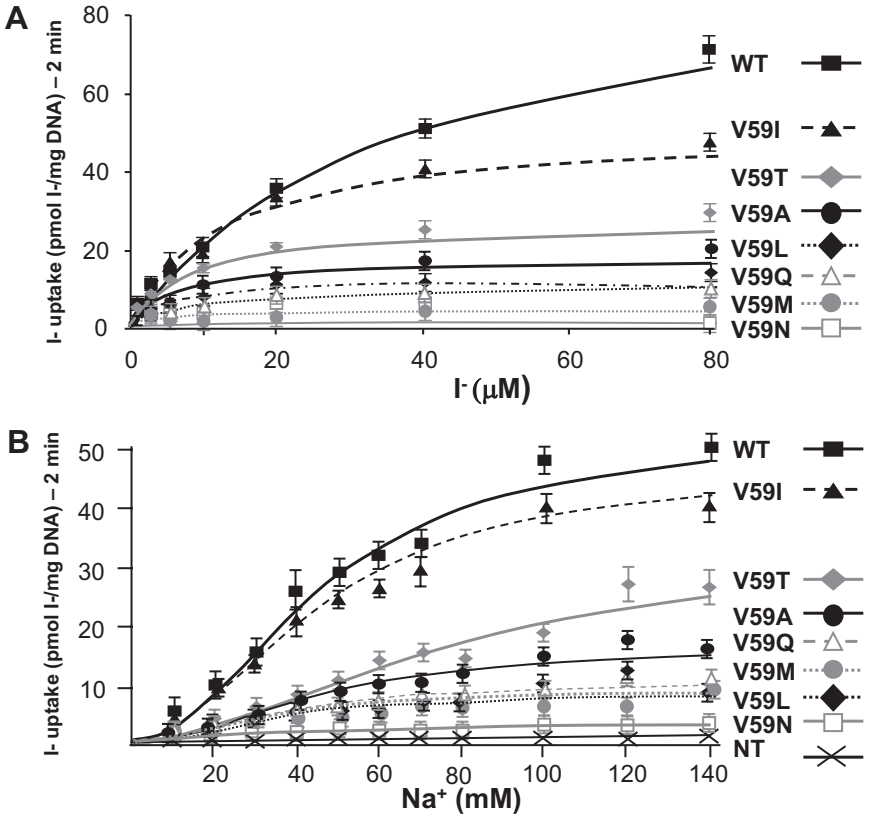

C

	Iodide Dependent Kinetic			Sodium Dependent Kinetic			
	Vmax (pmol I-/mg DNA)	Km (μM)	SE	Vmax (pmol I-/mg DNA)	Km (mM)	SE	Branch
WT	225	26 ± 5		65	57 ± 13		β-carbon
I	150	14 ± 2		42	60 ± 6		β-carbon
T	102	16 ± 4		43	87 ± 10		β-carbon
A	52	9 ± 2		18	65 ± 17		None
Q	37	11 ± 2		14	55 ± 15		δ-carbon
L	32	17 ± 6		19	47 ± 14		γ-carbon
M	21	10 ± 3		8	44 ± 14		None
N*	27	17 ± 8		4	20 ± 6		γ-carbon

FIG. 5. A, I^--dependent kinetic assays. cDNA constructs encoding WT NIS or NIS with amino acids at position 59 that were conducive to activity (V59A, I, L, M, N, Q, and T) were assayed for initial I^- transport rates (2 min) as a function of different I^- concentrations, ranging from 0.6125–80 μM, at a constant Na^+ concentration of 140 mM Na^+. V_{max} and K_m values were calculated with the equation $v([I^-]) = (V_{max} \times [I^-])/(K_m + [I^-]) + A \times [I^-] + B$ and the gnuplot program. B, Na^+-dependent kinetic assays. Cells were assayed to determine the initial rates of I^- transport as a function of the external $[Na^+]$. Cells were assayed for initial I^- transport rates (2 min) as a function of different Na^+ concentrations, ranging from 0–140 mM, at a constant I^- concentration of 20 μM. Results were analyzed using the gnuplot program and applied to the equation $v([Na^+]) = (V_{max} \times [Na^+]^2)/(K_m^2 + [Na^+]^2) - A \times [Na^+] + B$ to determine V_{max} and K_m. C, Average K_m (I^- and Na^+) and V_{max} (I^- and Na^+) values as determined by kinetic analysis. The table lists the average K_m and V_{max} values from six I^--dependent kinetic assays (*left*) and six Na^+-dependent kinetic assays (*middle*); in each experiment, activity was analyzed in triplicate. On the *right*, the position of the amino acid side chain of each amino acid is listed. The variation in V_{max} and the lack of significant variation of K_m values indicate that the decreased levels of I^- accumulation are not due to a change in the apparent affinity of the mutant NIS proteins for Na^+ or I^-. Interestingly, the amino acids that are branched at the β-carbon (such as Ile or Thr), *i.e.* equal to Val, accumulated the highest levels of I^-. Graphs in A and B correspond to a representative experiment.

ficiency of the mutant NIS constructs into COS-7 cells was measured by FACS analysis (not shown). An immunoblot of the cell lysates showed that the cotransfected NIS cDNA constructs were expressed at levels similar to WT NIS (Fig. 6A). Comparison of the signals visualized by immunoblotting the membrane proteins after cell surface biotinylation indicated that the mature polypeptides expressed after cotransfection reached the plasma membrane at amounts comparable to those of WT NIS (Fig. 6B). Still, we observed no I^- accumulation in COS-7 cells expressing V59E/T354P NIS, a finding consistent with the patients' phenotypes (Fig. 6C).

Discussion

The V59E NIS mutation was identified in three siblings in Japan (10, 24). The patients were heterozygous for both the T354P NIS mutation (inherited from their mother) and the V59E NIS mutation (inherited from their father). The three siblings had ITD, whereas their parents were healthy, compatible with the autosomal recessive character of ITD. Fujiwara *et al.* (10) cotransfected HEK293 cells with cDNA constructs encoding V59E and T354P NIS and reported 20% of WT NIS I^- transport in these cells, whereas HEK293 cells expressing V59E NIS transported almost 30% of WT NIS I^- transport. However, in the absence of I^- transport experiments in nontransfected cells and without a study of the effect of ClO_4^- in NIS-transfected cells, it is not possible to discriminate between NIS-mediated I^- uptake and nonspecific I^- binding and/or transport. In addition, the levels of expression of the different NIS proteins were not determined. Without this information, it is not feasible to accurately as-

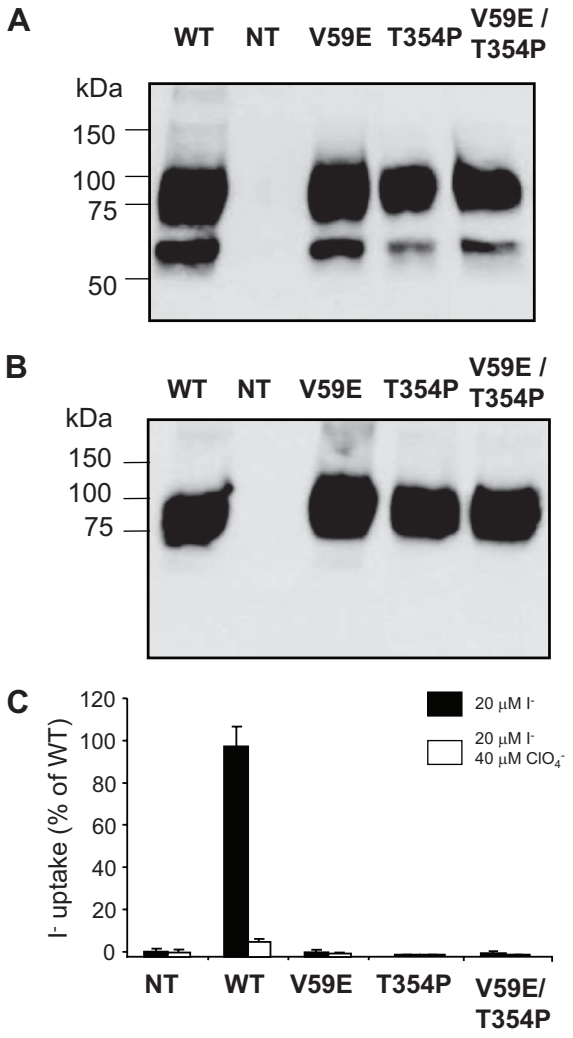

FIG. 6. Expression, plasma membrane targeting, and activity of V59E/T354P NIS. A, Immunoblot analysis. Cell lysates (2 μg) from COS-7 cells cotransfected with 2 μg each of V59E and T354P or transfected with 4 μg WT NIS were subjected to SDS-PAGE and immunoblotted with 2 nM anti-rNIS. B, Cell surface biotinylation. C, I^- uptake. V59E and T354P NIS cDNA (2 μg each) were cotransfected into COS-7 cells, and I^- accumulation was compared with that of V59E, T354P, or WT NIS cDNA (4 μg). Shown is I^- transport in cells incubated with 20 μM I^- and 140 mM Na^+ (*black bars*) or with 20 μM I^-, 140 mM Na^+, and 40 μM ClO_4^- (*white bars*). Values are a percentage of WT NIS activity. Values represent the average of at least three different experiments; in each experiment, activity was analyzed in triplicate.

sess NIS-mediated (*i.e.* Na^+-dependent, ClO_4^--inhibitable) I^- transport.

These authors' findings regarding the partial activity of V59E NIS contrast with our own observation that this mutant is inactive (Fig. 2), which is fully consistent with the lack of active I^- transport reported in the thyroid and salivary glands of the patients (24). The patients in whom the V59E NIS substitution was identified also carry the previously characterized T354P NIS substitution (22). Because ITD is an autosomal recessive disease and the three patients have ITD, both mutant NIS alleles inherited by the children must be inactive. Indeed, we have characterized the V59E NIS protein and determined that it is intrinsically inactive. Based on previous studies of some ITD-causing mutations, possible explanations for the inactivity caused by the replacement of Val with Glu include an inability to properly process and/or target the mutant protein to the plasma membrane (20) or a decreased ability to catalyze I^- transport owing to the difference in size and/or charge of the amino acid replacement (19, 21, 22); we investigated each of these possibilities.

Here we present a thorough analysis of the V59E NIS mutation and report that it renders NIS inactive because of the presence of the charged amino acid Glu, despite proper protein expression and plasma membrane targeting (Fig. 2). Furthermore, neutral amino acids branched at the β-carbon (Val, Ile, and Thr) and Ala were most conducive to NIS transport, compared with the other neutral amino acids that were substituted (Leu, Met, Gln, and Asn) (Fig. 4), whereas the presence of a charged amino acid prevented NIS activity, as did Pro (this result is most likely due to a bend in α-helix formation) (Fig. 3). Lastly, we determined that the reduction in I^- transport observed in the mutant NIS molecules that are capable of transporting I^- (V59A, I, L, M, N, Q, and T) was due to a decrease in NIS kinetic turnover, as opposed to a change in the apparent affinity of the transporter for Na^+ or I^- (Fig. 5).

According to our proposed secondary structure model (Fig. 1) (27), V59 is located in TMS II, close to the interface with the cytosol. The best explanation for our experimental data is that V59 is involved in intramembrane helix-helix contact. Given that all NIS mutants with substitutions at position 59 reached the cell surface, we conclude that charged residues at this position do not seem to affect correct folding and targeting; however, charged residues rendered NIS inactive, suggesting that accommodation of a charge of either polarity requires a large realignment of the two contacting helices so as to allow the charge to be compensated by a mobile charge at the membrane-cytosol interface. Replacements of V59 with neutral amino acids resulted in different levels of NIS activity, except for Pro, which rendered the protein inactive, most likely due to a disruption in α-helix formation (28). On the other hand, the activity elicited by the other neutral residue substitutions cannot be explained on the basis of their helical propensity properties, which relate to the relative stability of helices having different amino acids at a particular position, given that Met has long been recognized as a strong helix former (30). In general terms, small (Ala) and β-branched (Val, Ile, and Thr) residues led to higher NIS activity, probably because they allow the WT orientation of the helices to be preserved, whereas larger residues (Leu, Met, Gln, and Asn), although still yielding active proteins, led to lower NIS activity, probably because of a small rearrangement of the two helices involved. Elucidation of the three-dimensional structure of NIS would clarify the nature of the proposed helix-helix interactions.

The question remains as to how to explain the marked differences among the three siblings in phenotype and their improvement in thyroid function and clinical condition after treatment with KI. Fujiwara *et al.* (10) implicitly argue that when NIS function is diminished, excess I^- supply could compensate for the decreased transport capacity of NIS, and that differences in dietary I^- content could account for the

variability in phenotypes as observed in the three siblings (10). Their statement that NIS activity was not completely abolished is, as stated above, not compatible with the saliva/plasma I^- ratios of approximately 1, as found in all three patients. The clinical diagnosis of absence of NIS-mediated I^- uptake, experimentally proven by the complete lack of I^- transport mediated by the same NIS mutants when transfected into COS-7 cells, leaves no other conclusion than that other mechanisms of I^- entry into the thyroid must be present. The KI treatment that the siblings received (14 mg KI/d) is approximately 100 times the World Health Organization-recommended daily dietary I^- supply (150 μg/d) (30). In addition, Toyoshima *et al.* (24) stated that the Japanese diet has a median daily I^- content of 1.5 mg/d (24). Assuming a distribution volume of I^- of about 2.5 liters in children, the plasma I^- concentration in the siblings would have been approximately 164 μM, compared with 0.88 μM in adults in Western countries. It cannot be ruled out that at those high plasma I^- concentrations, other channels or transporters such as Cl^- channels or cystic fibrosis transmembrane conductance regulator (CFTR) may transport I^- into the thyroid (31, 32). Even then, it is remarkable that this bypass apparently leads to sufficient thyroid hormone production and physical development in the absence of NIS.

Toyoshima *et al.* (24) reported that the mother of the three siblings consumed large quantities of laminaria, a dried kelp that contains 302 mg I^-/100 g. Interestingly, there was a strong correlation between the severity of the ITD symptoms in the three siblings and their feeding habits during infancy. The two oldest siblings exhibited symptoms of ITD that were significantly less severe than those of the youngest sibling. The oldest sibling was fed only the mother's milk, which contained I^- (because NIS is expressed in the lactating mammary gland) (6), and had the least severe ITD symptoms. The middle sibling was fed a combination of the mother's milk and cow's milk and exhibited symptoms less severe than those of the youngest sibling, who was fed only cow's milk. Interestingly, it seems that the large quantities of laminaria consumed by the mother provided the two oldest children enough I^- to produce T_3 and T_4, as did the 14-mg doses of KI that were taken later in life.

Our studies show that V59E NIS is inactive (as is T354P NIS). The ITD symptoms observed in the siblings were ameliorated after treatment with high doses of I^-, first with the two older siblings whose cases of ITD were mild because of high I^- concentrations in their diet as infants and later in life to the 14 mg KI treatment, suggesting that when plasma I^- levels are extremely high, I^- enters the thyroid by way of other channels or transporters.

In summary, we have thoroughly analyzed V59E NIS and V59E/T354P NIS and determined that the presence of a charged residue at position 59 in NIS completely impairs I^- transport. We determined that the structural requirement at that position is a branched residue to allow proper helix-helix contact and the correct NIS kinetic turnover number. The patients' clinical data published by Toyoshima *et al.* (24) indicate that the severity of the symptoms in each child was related to whether or not and for how long they were breastfed. This observation underscores the importance of providing adequate amounts of I^- to infants, whether in maternal milk or formula, to ensure normal physical and mental development.

Acknowledgments

We thank the members of the Carrasco laboratory and Dr. J. Smit for critical reading of the manuscript.

Received January 9, 2008. Accepted March 3, 2008.

Address all correspondence and requests for reprints to: Nancy Carrasco, Albert Einstein College of Medicine, Department of Molecular Pharmacology, 1300 Morris Park Avenue, Bronx, New York 10461. E-mail: carrasco@aecom.yu.edu.

This work was supported by National Institutes of Health Grants DK41544 and CA098390 (to N.C.). M.R.-T. was supported by National Institutes of Health Grant 5T32 GM 07491 and a supplement of Grant CA098390. A.D.V. was supported in part by Grant FIS-ISCIII (PI061231 and RD06/0020/0060) from Spain.

Present addresses for A.D.l.V.: Instituto de Investigaciones Biomédicas "Alberto Sols" (Consejo Superior de Investigaciones Científicas), c/Arturo Duperier 4, 28029 Madrid, Spain 28029.

Present address for C.S.G.: Department of Physiology and Biophysics, Cornell Weill Medical College, New York, New York 10021.

Disclosure Statement: The authors have nothing to disclose.

References

1. **Carrasco N** 1993 Iodide transport in the thyroid gland. Biochim Biophys Acta 1154:65–82
2. **Eskandari S, Loo DD, Dai G, Levy O, Wright EM, Carrasco N** 1997 Thyroid Na^+/I^- symporter. Mechanism, stoichiometry, and specificity. J Biol Chem 272:27230–27238
3. **Dai G, Levy O, Carrasco N** 1996 Cloning and characterization of the thyroid iodide transporter. Nature 379:458–460
4. **De la Vieja A, Dohan O, Levy O, Carrasco N** 2000 Molecular analysis of the sodium/iodide symporter: impact on thyroid and extrathyroid pathophysiology. Physiol Rev 80:1083–1105
5. **Dohan O, De la Vieja A, Paroder V, Riedel C, Artani M, Reed M, Ginter CS, Carrasco N** 2003 The sodium/iodide symporter (NIS): characterization, regulation, and medical significance. Endocr Rev 24:48–77
6. **Tazebay UH, Wapnir IL, Levy O, Dohan O, Zuckier LS, Zhao QH, Deng HF, Amenta PS, Fineberg S, Pestell RG, Carrasco N** 2000 The mammary gland iodide transporter is expressed during lactation and in breast cancer. Nat Med 6:871–878
7. **Wolff J** 1983 Congenital goiter with defective iodide transport. Endocr Rev 4:240–254
8. **Fujiwara H, Tatsumi K, Miki K, Harada T, Miyai K, Takai S, Amino N** 1997 Congenital hypothyroidism caused by a mutation in the Na^+/I^- symporter. Nat Genet 16:124–125
9. **Fujiwara H, Tatsumi K, Miki K, Harada T, Okada S, Nose O, Kodama S, Amino N** 1998 Recurrent T354P mutation of the Na^+/I^- symporter in patients with iodide transport defect. J Clin Endocrinol Metab 83:2940–2943
10. **Fujiwara H, Tatsumi K, Tanaka S, Kimura M, Nose O, Amino N** 2000 A novel hV59E missense mutation in the sodium iodide symporter gene in a family with iodide transport defect. Thyroid 10:471–474
11. **Kosugi S, Bhayana S, Dean HJ** 1999 A novel mutation in the sodium/iodide symporter gene in the largest family with iodide transport defect. J Clin Endocrinol Metab 84:3248–3253
12. **Kosugi S, Inoue S, Matsuda A, Jhiang SM** 1998 Novel, missense, and loss-of-function mutations in the sodium/iodide symporter gene causing iodide transport defect in three Japanese patients. J Clin Endocrinol Metab 83:3373–3376
13. **Kosugi S, Okamoto H, Tamada A, Sanchez-Franco F** 2002 A novel peculiar mutation in the sodium/iodide symporter gene in Spanish siblings with iodide transport defect. J Clin Endocrinol Metab 87:3830–3836
14. **Kosugi S, Sato Y, Matsuda A, Ohyama Y, Fujieda K, Inomata H, Kameya T, Isozaki O, Jhiang SM** 1998 High prevalence of T354P sodium/iodide symporter gene mutation in Japanese patients with iodide transport defect who have heterogeneous clinical pictures. J Clin Endocrinol Metab 83:4123–4129
15. **Pohlenz J, Medeiros-Neto G, Gross JL, Silveiro SP, Knobel M, Refetoff S** 1997 Hypothyroidism in a Brazilian kindred due to iodide trapping defect caused by a homozygous mutation in the sodium/iodide symporter gene. Biochem Biophys Res Commun 240:488–491
16. **Pohlenz J, Rosenthal IM, Weiss RE, Jhiang SM, Burant C, Refetoff S** 1998 Congenital hypothyroidism due to mutations in the sodium/iodide symporter. Identification of a nonsense mutation producing a downstream cryptic 3′ splice site. J Clin Invest 101:1028–1035
17. **Tonacchera M, Agretti P, de Marco G, Elisei R, Perri A, Ambrogini E, De Servi M, Ceccarelli C, Viacava P, Refetoff S, Panunzi C, Bitti ML, Vitti P, Chiovato L, Pinchera A** 2003 Congenital hypothyroidism due to a new deletion in the sodium/iodide symporter protein. Clin Endocrinol (Oxf) 59:500–506
18. **Szinnai G, Kosugi S, Derrien C, Lucidarme N, David V, Czernichow P, Polak**

M 2006 Extending the clinical heterogeneity of iodide transport defect (ITD): a novel mutation R124H of the sodium/iodide symporter gene and review of genotype-phenotype correlations in ITD. J Clin Endocrinol Metab 91:1199–1204

19. **De la Vieja A, Ginter CS, Carrasco N** 2004 The Q267E mutation in the sodium/iodide symporter (NIS) causes congenital iodide transport defect (ITD) by decreasing the NIS turnover number. J Cell Sci 117:677–687
20. **De la Vieja A, Ginter CS, Carrasco N** 2005 Molecular analysis of a congenital iodide transport defect: G543E impairs maturation and trafficking of the Na^+/I^- symporter. Mol Endocrinol 19:2847–2858
21. **Dohan O, Gavrielides MV, Ginter C, Amzel LM, Carrasco N** 2002 Na^+/I^- symporter activity requires a small and uncharged amino acid residue at position 395. Mol Endocrinol 16:1893–1902
22. **Levy O, Ginter CS, De la Vieja A, Levy D, Carrasco N** 1998 Identification of a structural requirement for thyroid Na^+/I^- symporter (NIS) function from analysis of a mutation that causes human congenital hypothyroidism. FEBS Lett 429:36–40
23. **De la Vieja A, Reed MD, Ginter CS, Carrasco N** 2007 Amino acid residues in transmembrane segment IX of the Na^+/I^- symporter play a role in its Na^+ dependence and are critical for transport activity. J Biol Chem 282:25290–25298
24. **Toyoshima K, Matsumoto Y, Nishida M, Yabuuchi H** 1977 Five cases of absence of iodide concentrating mechanism. Acta Endocrinol 84:527–537
25. **Smanik PA, Ryu KY, Theil KS, Mazzaferri EL, Jhiang SM** 1997 Expression, exon-intron organization, and chromosome mapping of the human sodium iodide symporter. Endocrinology 138:3555–3558
26. **Turk E, Wright EM** 1997 Membrane topology motifs in the SGLT cotransporter family. J Membr Biol 159:1–20
27. **Levy O, De la Vieja A, Ginter CS, Riedel C, Dai G, Carrasco N** 1998 N-linked glycosylation of the thyroid Na^+/I^- symporter (NIS). Implications for its secondary structure model. J Biol Chem 273:22657–22663
28. **Nilsson I, von Heijne G** 1998 Breaking the camel's back: proline-induced turns in a model transmembrane helix. J Mol Biol 284:1185–1189
29. **Pace CN, Scholtz JM** 1998 A helix propensity scale based on experimental studies of peptides and proteins. Biophys J 75:422–427
30. **de Benoist B, Andersson M, Egli I, Takkouche B, Allen H** 2004 Iodine status worldwide. WHO Global Database on Iodine Deficiency. Geneva: World Health Organization
31. **Chen TY** 2005 Structure and function of clc channels. Annu Rev Physiol 67:809–839
32. **Tabcharani JA, Linsdell P, Hanrahan JW** 1997 Halide permeation in wild-type and mutant cystic fibrosis transmembrane conductance regulator chloride channels. J Gen Physiol 110:341–354

***Endocrinology* is published monthly by The Endocrine Society (http://www.endo-society.org), the foremost professional society serving the endocrine community.**